

RLFlow: Optimising Neural Network Subgraph Transformation with World Models

Sean Parker
Computer Laboratory
University of Cambridge
Cambridge, UK
sjp240@cantab.ac.uk

Sami Alabed
Computer Laboratory
University of Cambridge
Cambridge, UK
sa894@cam.ac.uk

Eiko Yoneki
Computer Laboratory
University of Cambridge
Cambridge, UK
eiko.yoneki@cl.cam.ac.uk

Abstract—We explored the use of reinforcement learning (RL) agents that can learn to perform neural network subgraph transformations, without the need of expertly designed heuristics to achieve a high level of performance. Reducing compute requirements of deep learning models is a focus of extensive research and many systems, optimisations and just-in-time (JIT) compilers have been proposed to decrease runtime.

Recent work has aimed to apply reinforcement learning to computer systems with some success, especially using model-free RL techniques. Model-based reinforcement learning methods have seen an increased focus in research as they can be used to learn the transition dynamics of the environment; this can be leveraged to train an agent using the hallucinogenic environment, thereby increasing sample efficiency compared to model-free approaches. Furthermore, when using a world model as a simulated environment, batch rollouts can occur safely in parallel and, especially in systems environments, it overcomes the latency impact of updating system environments that can take orders of magnitude longer to perform an action compared to simple emulators for video games.

We propose a design for a model-based agent which learns to optimise the architecture of neural networks by performing a sequence of subgraph transformations to reduce model runtime. We show our approach can match the performance of state of the art on common convolutional networks and outperform those by up to 5% on transformer-style architectures.

I. INTRODUCTION

Recent modern software has key components that are underpinned by machine learning (ML) models, specifically, deep neural networks (DNN).

A common internal representation for neural networks inside deep learning frameworks is that of a computation graph; a directed acyclic graph where nodes represent a specific computation and edges the paths where data is transferred. It is a common optimisation practice to support graph substitutions. Frameworks such as TensorFlow [1] and PyTorch [2] automatically apply optimisations in an effort to reduce computation resources during inference.

Currently, majority of the optimisation in deep learning frameworks is performed using manually defined heuristics. TensorFlow [1], TensorRT [3], and TVM [4] perform substitutions to a computation graph by using rule-based strategies. For example, TensorFlow [1] uses 155 handwritten optimisations composed of 53,000 lines of C++. While such heuristics

are applicable for current architectures, network design is consistently evolving. Therefore, we require consistent innovation to discover and design rules that control the application of optimisations with guarantees that strictly improve efficiency. Such approach is difficult to scale. Eliminating the need for manual engineering work that is required to design and implement the heuristics for applying optimisations is a primary focus of our work.

Recent work, namely TASO [5], has shown the substitution of the subgraphs by replacing heuristics with an automatic cost-based search. However, such approaches may not fully explore the potential search space due to the lack of forward planning in cost-based optimisation. As a step towards resolving the issue of poor exploration, this work explores the use of reinforcement learning (RL). RL is an area of machine learning in which an agent learns to act optimally, given a state and a suitable reward function, through interactions with an environment.

In this work, we focus on the use of RL for the task of optimising deep learning graphs. Specifically, we focus on a model-based reinforcement learning which aims to learn a model of the environment in which they act. In our work, the network learns to model the dynamics of sub-graph transformations in a deep learning model as well as the impact on overall runtime of the model when executed on-device. Further, learning a model of the environment provides important benefits; for example, lookahead planning, low-cost state prediction and faster wall-clock training. We examine the use of world-models for learning the environment as well as training a controller inside a world model which removes the need of an expensive, time-consuming computer system to apply the chosen subgraph transformations.

RLFlow is a graph-net based neural network optimisation as an extension of TASO. The basic idea was to substitute TASO’s cost-based backtracking search and replace it with a RL-based optimisation. This enables it to generalise to large unseen graphs and thus, find better performing solutions than a backtracking search.

To summarize, our contributions are:

- Applies model-based reinforcement learning approaches to eliminate the need for human engineered graph optimisations in machine learning frameworks. We show

that our proposed method can improve runtime by up to 58% compared to current deep learning frameworks. Specifically,

- Provides a detailed discussion and analysis of our solution as well as comparison to the current state-of-the-art methods in published literature.
- Implemented a model-based RL agent and environment for jointly choosing the optimal substitution and substitution location.
- This work, to the best of our knowledge, is the first that has applied model-based reinforcement learning in optimising computation graphs to reduce hardware resource requirements.

II. BACKGROUND

A. Computation graphs for neural networks

Over the past decade, there has been a rapid development of various deep learning architectures that aim to solve specific tasks. Common examples include convolutional networks, for a variety of tasks such as object detection and classification, transformer networks, used for translation and generation of language, as well as recurrent networks that have shown to excel at exploiting long and short term trends in data.

Despite the improvements in the accuracy of machine learning (ML) models, the fundamental building blocks of deep learning models have remained largely unchanged. As the networks become more complex, it also becomes tedious to manually optimise the networks to reduce the execution time on hardware. Therefore, there is extensive work to automatically optimise the models, or alternatively, apply a set of hand-crafted optimisations according to pre-defined rules.

Computation graphs are a way to graphically represent both the individual tensor operations in a model, and the connections (or data-flow) along the edges between nodes in the graph. Figure 1 shows how the expression, $y = \text{ReLU}(\mathbf{w} \cdot \mathbf{x} + b)$, can be represented graphically as a computation graph.

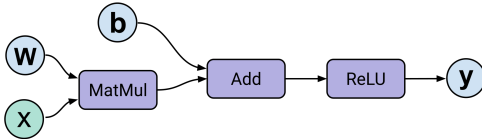


Fig. 1: The operations shown in purple are the nodes of the computation graph which take an arbitrary number of inputs, performs a computation at the node and produces an output. The blue nodes represent the input nodes for tensors. The directed edges show the flow of tensors through the graph.

Similarly, a complete neural network model can be converted into a stateful dataflow (computation) graph in this manner. Using a computation graph as an intermediate representation provides two key benefits compared to using a raw model definition. First, we can execute the model on any hardware device as the models have a single, uniform representation that can be modified as required. Second, it

allows for pre-execution optimisations based on the host device, for example, we may perform different optimisations for executing on a GPU compared to a TPU (Tensor Processing Unit) requires different data layouts and optimisations.

B. Reinforcement Learning

Reinforcement learning (RL) is a sub-field of machine learning, broadly, it aims to compute a control policy such that an agent can maximise its cumulative reward from the environment. It has powerful applications in environments where a model that describes the semantics of the system are not available and the agent must itself discover the optimal strategy via a reward signal.

Formally, RL is a class of learning problem that can be framed as a Markov decision processes (MDP) when the MDP that describes the system is not known [6]; they are represented as a 5-tuple $\langle \mathcal{S}, \mathcal{A}, \mathcal{P}_a, \mathcal{R}_a, \rho_0 \rangle$. \mathcal{S} is a finite set of valid states, \mathcal{A} , is a finite set of valid actions, \mathcal{P}_a , is the transition probability function that an action a in state s_t leads to a state s'_{t+1} . \mathcal{R}_a , is the reward function (it returns the reward from the environment after taking an action a between state s_t and s'_{t+1}) and finally, ρ_0 , is the starting state distribution.

We aim to compute a policy, denoted by π , that when given a state $s \in \mathcal{S}$, returns an action $a \in \mathcal{A}$ with the optimisation objective being to find a control policy π^* that maximises the *expected reward* from the environment as can be seen in (1). Importantly, we can control the ‘far-sightedness’ of the policy by tuning the discount factor $\gamma \in [0, 1)$. As γ tends to 1, the policy will consider the rewards further in the future but with a lower weight as the distant expected reward may be an imperfect prediction [6].

$$\pi^* = \arg \max_{\pi} \mathbb{E} \left[\sum_{t=0}^{\infty} \gamma^t \mathcal{R}_t \right] \quad (1)$$

Classic RL problems are formulated as MDPs in which we have a finite state space, however, such methods quickly become inefficient with large state spaces for applications such as Atari [7], [8] and Go [9]. Therefore, we take advantage of modern deep learning function approximators, such as neural networks, that makes learning the solutions far more efficient in practise. We have seen many successfully applications in a wide range of fields, for example, robotic control tasks [10], datacenter power management, device placement [11], [12], and, playing both perfect and imperfect information games to a super-human level [9], [13].

C. Motivation for Model-based RL

Model-free and model-based are the two main approaches to reinforcement learning, however, with recent work such as [8], [14], [15], the distinction between the two is becoming somewhat nebulous. It is possible to use a hybrid approach that aims to improve the sample efficiency of the agent by training model-free agents directly in the imagined environment.

The primary benefit of model-based RL is that it has greater sample efficiency, meaning, the agent requires in total less

interactions with the real environment than the model-free counterparts. If we can either provide or learn a model of the environment that enables the agent to plan actions an arbitrary number of steps ahead, the agent select from a range of trajectories by taking specific actions to maximise its reward. The agent that acts in this “imagined” or “hallucinogenic” environment can be a simple MLP [16] to a model-free agent trained using modern algorithms such as PPO [17], A2C [18] or Q-learning [7], [19]. Further, training an agent in the world model is comparatively cheap, especially in the case of complex systems environments where a single episode can be on the order of hundreds of milliseconds.

Unfortunately, learning a model of the environment is not trivial. The most challenging problem that must be overcome is that if the model is imperfect, the agent may learn to exploit the models deficiencies, thus the agent fails to achieve a high performance in the real environment. Consequently, learning an invalid world model can lead to the agent performing actions that may be invalid in an environment where not all actions are valid in all states.

Model-based RL approaches have been applied in a range of environments such as board games, video games, systems optimisation and robotics with a high degree of success. Despite the apparent advantages of model-based RL with regards to reduced computation time, model-free reinforcement learning is by far the most popular approach and massive amounts of compute. Typically, the models are trained on distributed clusters of GPUs/TPUs; large amounts of compute is required overcome the sample inefficiency of model-free algorithms.

III. RLFLOW

A. Reinforcement Learning Formulation

1) *System environment*: In order to train a reinforcement learning agent, it necessary that we have access to an environment that, given the current environment state, the agent can take an action. After taking the chosen action, the environment is updated into a new state and the agent receives a reward signal. Typically, one uses a mature environment such as OpenAI Gym [20] or OpenSpiel [21] as the quality of the environment often has a significant impact on the stability of training. Moreover, using an environment that uses a common interface allows researchers to implement algorithms with ease, and importantly, reproduce results from prior work.

In our work, we implemented an environment that follows the OpenAI Gym API standard stepping an environment, that is, we have a function `step(action)` that accepts a single parameter, the action requested by the agent to be performed in the environment. The `step` function returns a 4-tuple (`next_state`, `reward`, `terminal`, `extra_info`). `extra_info` is a dictionary which can store arbitrary data.

To simplify the implementation of the environment, we used made extensive use of the work by Jia et al. [5] with the open source version of TASO. We provide a computation graph and the chosen transformation and location; TASO then applies the requested transformation and returns the newly transformed

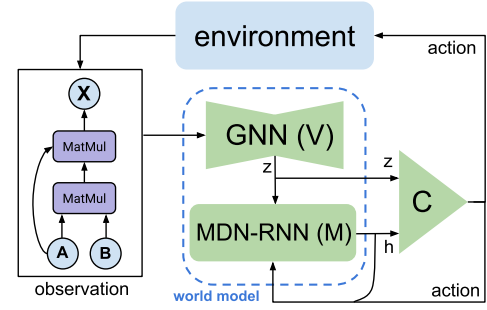


Fig. 2: Data flow between components of the system. We select an action given the current state of the imagined environment in the World Model.

graph. Further, we use internal TASO functions that calculates estimates of the runtime on the hardware device which we use as our reward signal for training the agent. During our experiments we modified TASO to extract detailed runtime measurements to analyse the rewards using a range of different reward functions—we provide more detail in Section III-A3.

2) *Computation Graphs*: The first step prior to optimising a deep learning graph is that we must load, or create on-demand, the model in a supported deep learning framework. In our project, we can support any model that can be serialised into the ONNX [22] binary format which is a open-source standard for defining the structure of deep learning models. By extension, we can support any deep learning framework that supports serialisation of models into the ONNX format such as TensorFlow [1], PyTorch [2] and MXNet [23].

Next, we parse the ONNX graph representation by converting all operators into the equivalent TASO tensor representations such that we can modify the graph using the environment API as we described in Section III-A1. Although our environment does not support the conversion of all operators defined in the ONNX specification¹, the majority of the most common operators are supported.

3) *Reward function*: The design of a reinforcement learning agent consists of three key elements, the agent, environment and reward function. Most importantly, we require a reward function that captures dynamics of the environment in such a way that we can directly indicate to the agent if we consider the action to be “good” or “bad”. For example, we wish to prevent the agent from performing actions that would be invalid in the environment, therefore, using the reward signal we provide a large negative reward to disincentivize the agent from replicating the behaviour. Conversely, we need to provide a positive reward, that is calculated using the chosen action and its impact on the agent performance.

Selecting optimal actions can be challenging in any deep reinforcement learning system, especially those with either long-term action dependencies or a large number of possible actions in any given state. Importantly, in our environment,

¹ONNX operator specification: <https://github.com/onnx/onnx/blob/master/docs/Operators.md>

the selection of a poor action be impactful on both subsequent action space and the resulting reward generated by the environment. Therefore, we used multiple reward functions to investigate the resulting performance of the agent. First, we used a simple reward function that is commonly used in sequential RL applications:

$$r_t = \begin{cases} RT_{t-1} - RT_t, & \text{if valid action} \\ -100, & \text{otherwise} \end{cases}$$

Using the reward function defined above, we use the previous estimated runtime, RT_{t-1} of the computation graph and the estimated runtime of the current graph, RT_t , to determine the step-wise, incremental change in graph runtime as the reward. This simple, yet powerful function has the benefit of a very low overhead as we only need to store the last runtime. Furthermore, as our primary goal is to reduce the execution time of the graphs, rather than for example the system memory, it directly captures our desired metric which we wish to optimise.

Secondly, we instrumented TASO to extract detailed metrics in an attempt to engineer a more complex reward function; we used the runtime, FLOPS, memory accesses and kernel launches to perform experiments to determine if using a combination of the metrics could yield a higher performance RL agent. We defined modified reward function as shown below; where RT is the graph runtime, M is the memory accesses, α and β are two hyperparameters for weighting the runtime and memory accesses respectively.

$$r_t = \begin{cases} \alpha(RT_{t-1} - RT_t) + \beta(M_{t-1} - M_t), & \text{if valid action} \\ -100, & \text{otherwise} \end{cases}$$

We provide further discussion and motivation for our chosen reward functions in Section IV-D as well as an analysis of the detailed runtime metrics and the impact on graph runtime.

B. Graph-level optimisation

Performing optimisations at a higher, graph-level means that the resulting graph is—in terms of execution methodology—no different than the original graph prior to optimisation. Therefore, by performing graph-level optimisation we generate a platform and backend independent graph representation which can be further optimised by specialised software for custom hardware accelerators such as GPUs and TPUs.

Next, we define that two computation graphs, \mathcal{G} and \mathcal{G}' are semantically equivalent when $\forall \mathcal{I} : \mathcal{G}(\mathcal{I}) = \mathcal{G}'(\mathcal{I})$ where \mathcal{I} is an arbitrary input tensor. We aim to find the optimal graph \mathcal{G}^* that minimises a given cost function, $\text{cost}(\mathcal{G})$, by performing a series of transformations to the computation graph at each step, the specific transformation applied does not need to be strictly optimal. In fact, by applying optimisations that reduce graph runtime we further increase the state space for the search; a large state space is preferable in the reinforcement learning domain.

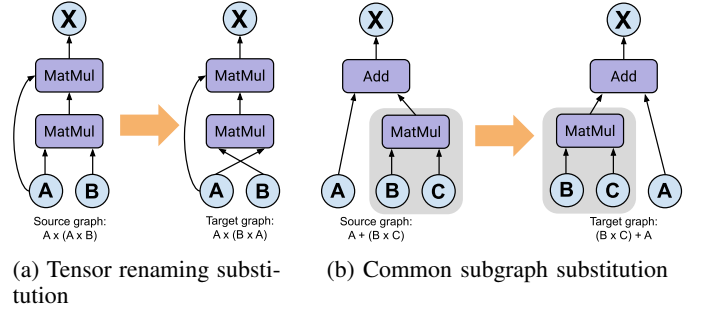


Fig. 3: Two examples of trivial graph substitutions that does not impact the overall runtime of the computation graph. The left sub-figure shows a simple renaming of the tensor inputs. The figure on the right shows that we have a common sub-graph between the source and the target graphs. In both cases we eliminate the duplicates as the hash of the two graphs will be identical.

In this work, we take the same approach as that of TASO and automatically generate the candidate sub-graphs. We perform this as an offline step as it requires a large amount of computation to both generate and verify the candidate substitution; to place an upper bound on the computation, we limit the input tensor size to a maximum of $4 \times 4 \times 4 \times 4$ during the verification process. Following the generation and verification steps, we prune the collection to remove substitutions that are considered trivial and as such would not impact runtime. For example, trivial substitutions include input tensor renaming and those with common sub-graphs. We show both techniques diagrammatically in Figure 3a and 3b respectively.

C. World Models

World models, introduced by Ha et al. [16], create an imagined model of the true environment by observing states, actions and rewards from the environment and learning to estimate the transitions between states based upon the actions taken. Ha et al. showed that the world models can learn the environment transitions and achieve high performance on visual learning tasks such as CarRacing and VizDoom that exceeds that of model-free agents. One should note that Ha & Schmidhuber used RGB pixel images as input to a convolutional neural network to generate the latent space embedding. In comparison, we used the latent space produced by the graph neural network using the graph as input. In either case, we aim to learn the world model using the latent space from the environment.

1) *Recurrent Neural Networks*: Recurrent Neural networks (RNNs) are a class of architectures in which the connections between the nodes form a directed graph in a temporal sequence [24]. Importantly, as the output of an RNN is deterministic, we use the outputs from the RNN as the parameters for a probabilistic model to insert a controllable level of stochasticity in the output predictions; a method first proposed by Graves [25].

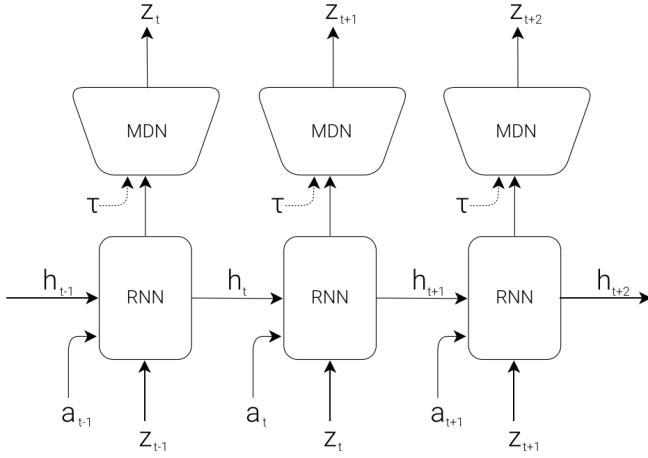


Fig. 4: Structure of an unrolled MDN-RNN. The MDN-RNN generates an output which is used as the parameters of a Gaussian mixture distribution. The parameterised GMM is then used to sample the distribution for the vector z_{t+1} ; the MDN is controlled by the temperature parameter τ . Adapted from [16].

A constraint of using RNNs is that they expect a fixed sized input sequence. However, in our work, both the shape of the latent state tensor, and the number of actions performed by the agent in a rollout is variable. As such, we employ a common approach to mitigate this problem is by appending zero values to the input sequence until the desired length is reached, this approach is commonly referred to as padding. After performing inference on the model and retrieving the predicted state, we mask the results based on the input padding to ensure we only use valid predictions to select the next action using the controller.

2) *MDN-RNN*: By combining the mixture density and recurrent networks, we can use rollouts of the environment sampled using a random agent to train the combined network, called an MDN-RNN. We use the network to model the distribution $P(z_{t+1} | a_t, z_t, h_t)$, where z_t and z_{t+1} is the latent state at the times t and $t + 1$ respectively, a_t is the action performed at time t , and h_t is the RNN networks hidden state at time t . Figure 4 shows the combination of the RNN and MDN networks and how we calculate the predictions of the next latent state in sequence.

Furthermore, after training the world model, we must train an agent (or controller) to perform actions in the world model and learn to take optimal actions that maximise reward. During inference of the world model, we use a softmax layer which outputs π in the form of a categorical probability distribution which we sample under the Gaussian model parameterised by (μ_i, σ_i) .

In Figure 4 we show that one of the inputs to the MDN is τ , the temperature. By altering the temperature it allows us to control the stochasticity of the agent during training of the controller. The logits of the RNN that represent the predictions for the values of π are divided by the temperature prior to be-

ing passed into the softmax function which converts the logits into pseudo-probabilities. We incorporate the temperature, τ , into the function using the following equation.

$$\text{softmax}(\mathbf{x}_i) = \frac{\exp\left(\frac{x_i}{\tau}\right)}{\sum_j \exp\left(\frac{x_j}{\tau}\right)}$$

Typically, temperature is a real number in the range $\tau \in [0, 1)$, where a value of zero leads to completely deterministic predictions generated by the RNN, whereas larger values introduces a greater amount of stochasticity in the predictions. As larger values of τ increases the probability of samples with a lower sampling likelihood being selected it leads to a greater diversity of actions taken by the agent in the environment. Importantly, Ha et al. [16] found that having a large temperature can aid in preventing the agent from discovering strategies to exploit in the world model which are not possible true system environment due to an imperfect model.

Modifying the softmax activation function in this way is equivalent to performing knowledge distillation between two models; learnt information is transferred from a large teacher model, or ensemble model, to a smaller model which acts as a student model [26]. In both the context of knowledge distillation and training a controller network using the world model, a high temperature will generate a softer targets. Specifically, in this work a higher temperature produces a softer pseudo-probability distribution for π in the GMM. Additionally, using soft targets will provide a greater amount of information for the model to be learn by forcing the model to learn more aggressive policies, thus outputting stochastic predictions which is beneficial to encourage exploring the environments state-action space.

Furthermore, we consider how the world model is trained. For any supervised learning task we require target data to which we can compare our predictions, calculate a loss and perform backpropagation to update the weights in the network. To train the world model, we use a random agent, one that has an equal probability of choosing any action from the valid set of actions in a given state. Unlike Ha and Schmidhuber [16] who performed 10,000 rollouts of the environment offline using a random policy to collect the data, we took a different approach.

Rather than generating large rollouts offline, we generated minibatch rollouts using the random agent online, and directly used the observations to train the world model. Although this approach reduces the data efficiency as we only use each state observation once, we benefit from removing the need to generate the data prior to training. In systems environments, it is often expensive—in terms of computation time—to step the environment collect a diverse dataset.

D. Action Controller

Finally, we discuss the design of the “controller”, the network/agent that learns to output actions based upon the output from the MDN-RNN world model. Ha and Schmidhuber [16] used an evolution based controller defined as a simple

multi-layer-perceptron, $a_t = W_c[z_t, h_t] + b_c$, that accepts the hidden and current states from the recurrent network to predict the next action to be taken. A challenge when training the controller inside the fully imagined world environment is that we no longer have access to the ground truth state nor the reward produced by the real environment, therefore, we cannot use supervised learning to train the controller.

In [16] the authors used an evolutionally algorithm, covariance matrix adoption evolution strategy (CMA-ES) [27], which optimises the weights of the network based on the reward produced by the world model. Alternatively, recent work by Hafner et al. [28], [29] has shown to achieve state-of-art results in the Atari environment using an actor-critic method as the controller in the world model. Furthermore, prior work on the application of world models to systems environments has shown one can train a model-free controller inside the world environment [14].

IV. EVALUATION

A. Aims

In this section, we look to assess aims we presented at the beginning of this work where we claimed to use reinforcement learning to perform automated optimisation of deep learning computation graphs. Thus, this evaluation seeks to answer the following questions:

- 1) Are model-based reinforcement learning methods able to model the transition dynamics of the environment?
- 2) Do the world models accurately model the reward estimation from the graphs latent state?
- 3) Are the agents trained in an imagined world model applicable to the real-world environment?

Throughout this section, we aim to answer these questions by a series of experiments which provide evidence to support our claims. Finally, we conclude with an overall discussion of our findings and its impact.

B. Experimental Setup

All the experiments presented were performed using a single machine running Ubuntu Linux 18.04 with a 6-core Intel i7-10750H@2.6GHz, 16GB RAM and an NVIDIA GeForce RTX 2070.

To interface with the internal representation of the computation graphs, as previously discussed, we used the open-sourced version of TASO [5] which we modified to extract detailed runtime information. Further, we implemented the reinforcement learning algorithms in TensorFlow [1] and utilised the `graph_nets` package developed by Battaglia et al. [30] to process our input graphs using the method which we described in Section III-A1. The PPO agent was implemented based upon the implementation provided by Schulman et al. [17].

C. Graphs Used

We chose to use six real-world deep learning models to evaluate our project. InceptionV3 [31] is a common, high-accuracy model for image classification trained on the Im-

Graph	Type	Layers	Unique Layers	Substitutions
InceptionV3	Convolutional	43	12	56
ResNet-18	Convolutional	18	6	40
ResNet-50	Convolutional	50	6	228
SqueezeNet1.1	Convolutional	21	3	288
BERT-Base	Transformer	12	3	80
ViT-Base	Transformer	16	5	60

TABLE I: Properties of the six evaluation graphs used in the experiments contained in this chapter. We differentiate the total number of layers in a network from the number of unique layers used in composing the network to provide a more accurate representation of its complexity.

geNet dataset². ResNet-18 & ResNet-50 [32] are also deep convolutional networks that are 18 and 50 layers deep respectively. SqueezeNet [33] is a shallower yet accurate model on the same ImageNet dataset. BERT [34] is a recently introduced large transformer network that has been to improve Google search results [35]. Finally, ViT, a transformer network specifically designed for computer vision tasks; ViT [36] has been shown to outperform traditional convolutional networks at image recognition tasks. As these graph were also used in the evaluation of TASO [5], we can show a direct comparison of the performance between the different approaches.

D. Reward functions

As we described in Section III-A3, the design of the reward function used in the training of RL agents is a pivotal part of the agents architecture. In this section, we analyse our proposed reward functions and the effect on the convergence as well as final performance of the trained agents.

Figure 5 shows the pairwise relationship between the four detailed runtime measurements which we record at each step of the training process for the BERT graph. We collected the runtime, FLOPS, memory access and number of kernel launches and show the relationship between the quantities. We note that the estimated runtime and memory accesses have a strong correlation; when the memory access decreases, we see a notable decrease in estimated runtime.

Figure 6 shows the effect on convergence of model-free RL agents while training on the BERT graph using various reward functions. Significantly, using the approach of the first reward function as described in Section III-A3 shows that the model-free agent improves at a linear rate as shown by R4 in Figure 6. Whereas, using the second reward function and tuned hyperparameters of α and β , shown by R1, converges the fastest.

However, the rate of convergence does not show the whole picture of the agents performance. We note that the highest performing agent, after the restricted 500 epoch training time, was R1 with an average runtime improvement of $48.7 \pm 3.2\%$. Surprisingly, the second highest performing agent was the agent using R4, the simplest reward function from the set tested, with a performance of $43.2 \pm 2.3\%$.

²<https://image-net.org/index.php>

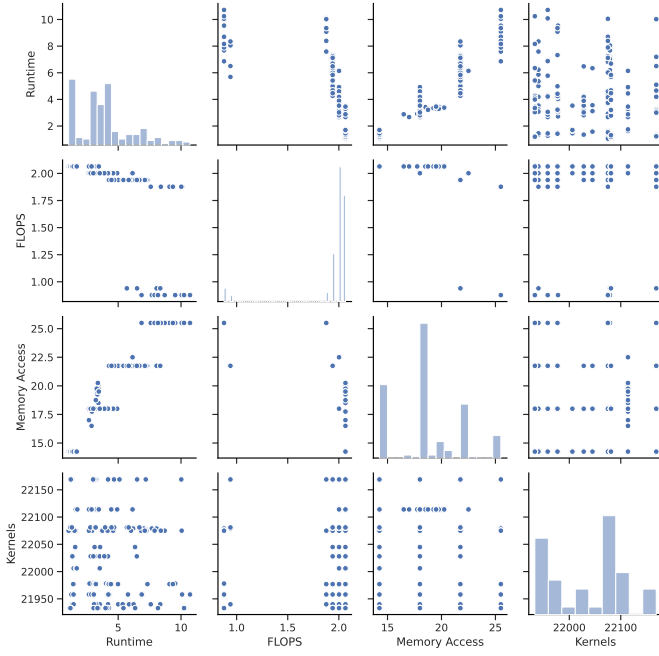


Fig. 5: Pairwise correlation between the detailed runtime metrics recorded directly from the TASO environment while training on the BERT graph. We note the strong correlation between the number of memory accesses and estimated runtime improvement.

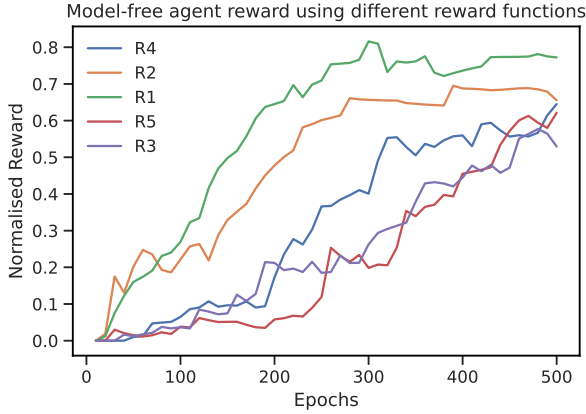


Fig. 6: Normalised reward of each agent using various reward functions while being trained for 500 epochs. R1 uses the second reward function with tuned parameters, R2 uses new runtime reward, R3 uses $\alpha = 0.1, \beta = 0.9$, R4 uses $\alpha = 0.5, \beta = 0.5$ and finally, R5 uses incremental runtime improvement.

In order to find the values of hyperparameters α and β which results in the agent with the maximum performance, we performed a grid search for α and $\beta = 1 - \alpha$ between the values of $[0, 1]$ in increments of 0.1. After training each agent for 500 epochs and evaluating the agents performance for five runs, we found that the reward function resulting in

the highest performance was using the values 0.8 and 0.2 for α and β respectively.

E. Runtime Performance

Figure 7 shows the runtime of the optimised graphs for the model-based agents trained inside the fully hallucinogenic world model. Each agent was trained inside a world model using rollouts from its respective graph as described in Section III-D. We trained the agents for a maximum of 1000 epochs, in mini-batches of 10 epochs. Additionally, we used a fixed learning rate for both the policy and value networks during training of the controller agent network.

Firstly, we note that training the agents on convolutional networks, especially SqueezeNet1.1 and InceptionV3, the model-based agent failed to outperform TASO, although we still decreased the runtime compared to the graph produced by TensorFlow optimisations. Importantly, we observe that the model-based agent outperformed all baseline approaches on the BERT transformer network; we improved the runtime by 54.1% and 7.3% compared to TensorFlow and TASO respectively. Figure 11 shows the transformations applied by the model-based agent on the test graphs and compared to TASO, we only apply a single transformation over 20 times—compared to TASO which uses four distinct transformations produce the optimised graph.

Compared to the strictly model-free agent that was trained using the real system environment, our model-based agent achieved a similar level of performance on the majority of the tested graphs. The model-free agent was trained for 2000 epochs and, by extension, over 4,000,000 interactions with the real environment. Comparatively, the model-based agent performed approximately 1,000,000 interactions with the real environment as the agent did not interact with the real environment while training inside the world model. Therefore, it is evident that by training inside the world model we improved the sample efficiency of the agent. On the other hand, the performance of the agent decreased compared to the model-free agent in four of the six tested graphs.

Furthermore, an important consideration when training inside a systems environment is the wall-clock time for stepping the environment to a new state based upon the agent action. We analysed the time required to perform a single step while training the ResNet50 graph. We found that stepping the world model (performing inference of the world-model) takes, on average, 10ms whereas stepping the real environment takes on average 850ms. Thus, although the performance of the model-based agent was comparatively lower, our wall-clock time for required for training was reduced by a factor of 85x.

Finally, we can observe that RLFlow has stronger performance when optimising transformer-based models compared to convolutional networks.

Transformers are becoming increasingly popular in both research and industry. They have not only been applied to Natural Language Processing (NLP), but Vision Transformers [36] (ViTs) provides strong performance, thus replacing traditional CNNs.

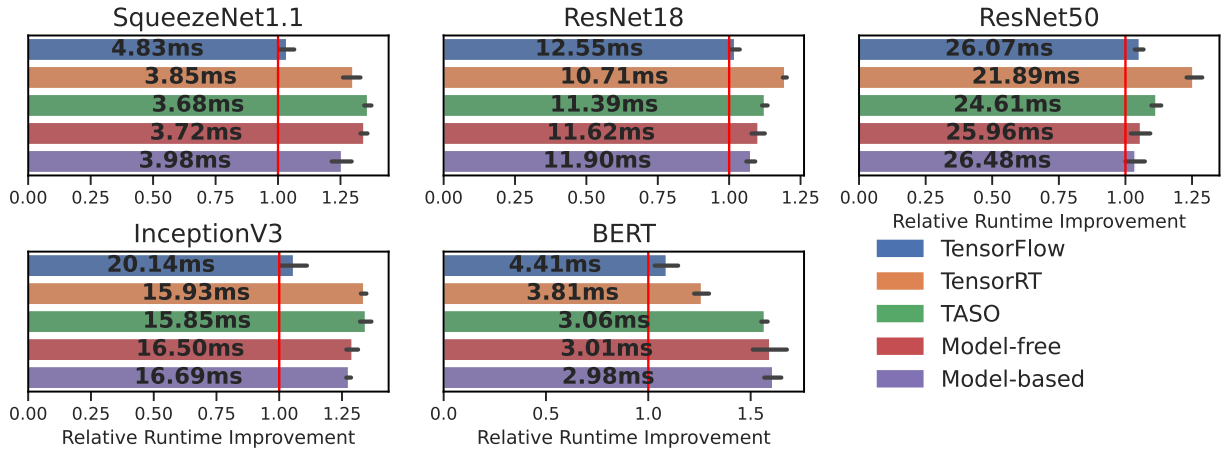


Fig. 7: Runtime of optimised graphs using an agent trained using the model-based world model. We also show the baseline results as comparison. The x-axis shows the relative runtime improvement, a higher relative runtime is better. Each experiment was performed five times; we report the mean inference time, and 95% CI through error bars.

F. Optimisation Time

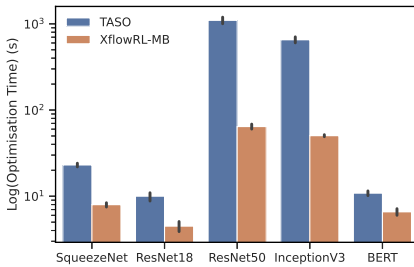


Fig. 8: Time required to generate the optimised model using model-based RL and TASO. In all cases, the optimisation time using our proposed approach is lower than that of TASO.

Figure 8 shows the optimisation time required to generate the optimised graph of the tested models. We note that the optimisation time for the model-based agent does not include the time required to learn the world model nor training the controller in the environment. The optimisation time is measured as the the wall-clock time to perform n agent steps to generate the optimised graph using our RL agents. Thus, although TASO has a longer optimisation time compared to the RL agent, TASO only requires us to perform the cost-based search a single time.

G. Memory Usage

Table II shows the percentage improvement of both the inference time and the memory used for performing inference on the optimised models. Importantly, although we only tasked the agent to optimise for reducing the runtime of the graphs, we observe a secondary effect in a reduction of memory usage by the model of up to 4.5%, compared to TensorFlow. Although this result is not unsurprising; optimising a models

TABLE II: Relative performance improvement of the graphs when optimised by RLFlow ($\tau = 1.0$) compared to TensorFlow

	TensorFlow		RLFlow	
	Inf. time (ms)	Mem. usage (GiB)	% Improvement	
ResNet18	12.55	1.18	5.2%	1.1%
ResNet50	26.07	2.34	-1.6%	0.6%
InceptionV3	20.14	2.11	17.1%	2.3%
SqueezeNet1.1	4.83	1.14	17.6%	1.8%
BERT-Base	4.41	0.26	32.4%	4.5%
ViT-Base	3.81	0.34	30.7%	3.2%

architecture leads to a smaller model in regards to number of trainable parameters. It shows that tasking the agent with reducing runtime does not come at the expense of other resources with strict usage constraints.

H. World-model accuracy

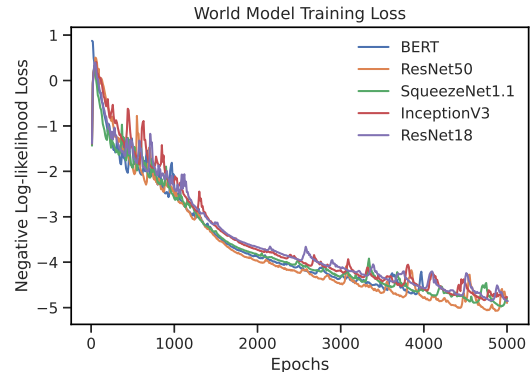


Fig. 9: Log-likelihood loss during training on each of the six graphs. The learning rate was decayed over the course of 5000 epochs using a 2nd-degree polynomial decay policy.

The training of the model-based agent is split into two parts. First, we train the world-model, the network that learns to simulate the environment dynamics, and secondly, we train the controller network inside the world-model. Figure 9 is a plot of the log-likelihood loss for each graph during training of the world model; it shows the convergence of the world model during training after approximately 5000 epochs on all graphs. We used the same hyperparameters for training each world model as well as decaying the learning rate over the course of 5000 epochs with a 2nd-degree polynomial decay policy. We note that despite all the graphs having different architectures, depths and transformation availability, the world model is able to generalise and learn to represent the transformation state transitions accurately after a short period of training. The MDN-RNN is trained with 8 Gaussians and 256 hidden units, all other hyperparameters used in training the MDN-RNN world model are the same as those used by Ha and Schmidhuber [16], unless otherwise stated.

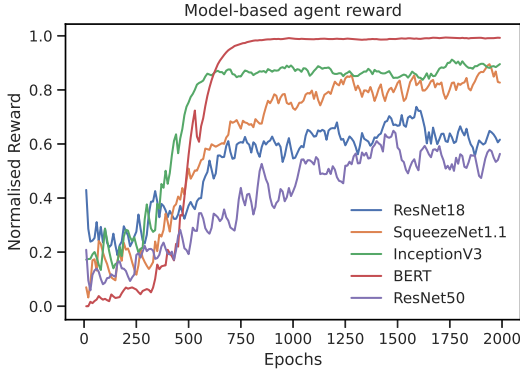


Fig. 10: Predicted reward produced by the world model while training the agent inside a the imagined environment. All rewards are normalised into the same range.

Figure 10 shows the reward (decrease in estimated runtime) for each graph as predicted by the world model during training. As the tested graphs have a wide range of epoch rewards, we perform min-max normalisation to scale the plots into the same range. This finding also supports the results shown in Figure 7. The agent applies higher performing optimisations to transformer networks (BERT-Base and ViT-Base) compared to convolutional networks. Notably, for all transformer networks, the optimal strategy is found after approximately 700 epochs.

On the contrary, networks such as ResNet 18/50 are less stable during training with a high epoch to epoch variation in rewards and we see that the agent struggles to learn an optimal sequence of subgraph transformations to apply.

If we assume that both the model-free and model-based agents should achieve a similar level of performance once trained, the results in Figure 10 shows that the agents trained in the world model are less stable. We hypothesise that there are three factors for such a discrepancy to occur:

- Imperfect world-model reward predictions leading to incorrect (or invalid) actions being performed

- Next state prediction by the world-model generating states that are invalid due to poor generalisation of the model
- Incorrect action mask predictions that would lead to a divergence between the world-model state and real environment state

In an attempt to resolve the issues highlighted above, we performed further experiments which we believe would aid in both reducing the variance in reward prediction as well as stabilise the world-model during training to prevent state divergence over time. We performed a temperature sweep of the hyperparameter τ which is used in training agent inside the world model, shown in Section IV-I.

I. Temperature Sweep

TABLE III: Temperature sweep of trained model-based agent optimising the BERT network. We show the percentage improvement of the models compared to TensorFlow in the scores produced by the world model and in the real environment. The highest performing model (over five runs) is shown in **bold**

Temperature	World-model Score	Real Score
0.1	6.67% \pm 0.6%	43.92% \pm 5.1%
0.5	7.75% \pm 0.3%	55.33% \pm 6.7%
0.75	9.10% \pm 0.4%	55.80% \pm 5.2%
1.0	8.85% \pm 1.2%	55.78 \pm 4.0%
1.2	9.91% \pm 0.8%	57.01% \pm 3.9%
1.5	10.20% \pm 0.6%	58.23% \pm 3.6%
1.75	9.92% \pm 1.0%	52.07% \pm 5.8%
2.0	9.65% \pm 0.8%	46.12% \pm 5.4%
2.5	10.04% \pm 2.0%	41.14% \pm 10.2%
3.0	10.38% \pm 1.9%	51.32% \pm 7.2%

Table III shows the results from performing a temperature sweep in which we used different values of τ while training the agent in a world model. After training, we evaluated the agent which produced an optimised graph that we evaluated to determine average runtime. The table shows the average reduction in runtime and standard deviation, averaged over five runs, compared to the unoptimised graph. The motivation for using a range of temperatures is that a higher value of τ leads to softer targets for the agent to predict, thereby improving generalisation. Conversely, a lower value of τ presents hard targets and thus when $\tau = 1.0$, it is equivalent to using the unmodified mixing weight, π , of the MDN.

Based upon the results in table III from the conducted experiments, we note that the world model agents are stable to temperatures within the range of $\tau = 0.5$ to $\tau = 1.75$. Although the runtime improvement world-model from the environment is consistently above 6%, we observe a large difference between the predicted runtime improvement and the real environment reward. One approach to producing more accurate reward predictions could be to use a separate reward prediction network such as those used by Brown et al. [14].

J. Graph transformations

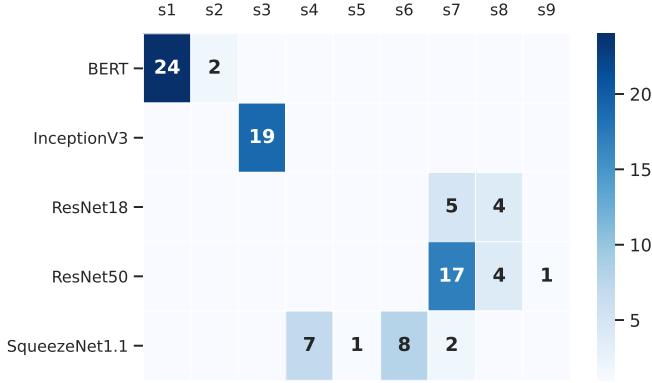


Fig. 11: Heatmap showing the transformations applied by the trained controller acting inside the world model. Although there are over 100 possible transformations, we only show the transformations applied onto at least one graph. The counts for each transformation shows the number of times it has been applied. A higher count means that RLFlow was able to find a long sequence of transformations before termination. This can indicate RLFlow has discovered a performant graph via the transformation sequence.

Figure 11 shows a heatmap of the various graph transformations which have been applied by a trained model-free agent during evaluation. Notably, the optimisations applied to the ResNet18/50 graphs apply similar transformations, those targeting the convolutions in the network; as the networks are composed of alike convolutional operators, with different depths, we apply analogous transformations. On the other hand, for recurrent networks such as BERT, we only apply relatively few transformations. This is in stark contrast to the series of transformations found by TASO which applies four distinct substitutions in comparison to the two applied by our approach.

As we can infer from Figure 11, and the results presented in TASO, there is a large difference between the two approaches in both the specific transformations and the number of times each was applied. Despite this difference, we found that our method can achieve similar levels of performance in convolutional networks and outperform TASO when optimising transformer-based networks. This primarily shows that there are many possible optimisation paths to achieve a performant, highly optimised network architecture.

K. Summary

In summary, as we have shown, the performance of a cost-directed search is largely dependent on the neural network architecture. Similarly, our approach performs better on specific architecture types (such as transformers), compared to convolutional networks. The cost-directed search method might be altered and the appropriate optimisation methods for transforming the subnetworks might be selected. For example, recent work by Wang et al. [37] has shown that using

architecture specific, approximate transformations can lead to higher performance gains compared to [5], [38].

V. RELATED WORK

Optimisation of computation graphs is the strategy by which we transform an input graph to alter its performance characteristics. Rule-based approaches such as those used in TensorFlow [1] and TVM [4] use a pre-defined set of transformations that are applied greedily. In addition, recent work, such as [5], [38] automatically search for transformations to apply to the input graph with the modification that we allow performance decreasing transformations. Their work is similar to our approach, as we use the same automated method to discover and verify the operator transformations in an offline manner—prior to optimisation of the models.

Model-based Reinforcement Learning is a class of reinforcement learning algorithms in which we aim to learn a model (or use a given model) of the real environment where an agent acts. The work in [16] proposed a novel approach to learn a “world model” using recurrent neural networks; we take inspiration from such work and use world models and a policy optimisation algorithm as the controller in the world model. In contrast, alternative approaches have been proposed such as imagination-augmented agents [39] and model-based value estimation for model-free agents [40]. Other work such as [15], [29] build discrete world models and train directly in latent space. Prior work on world models used a variation on a variational auto-encoders [16], [28] to generate a latent state of the pixel input, instead we use a graph neural network [30] to generate a latent representation of the input computation graphs.

RL in Computer Systems is a relatively recent topic of research. In recent years there has been an increased focus on using model-free RL in variety of systems environments. For example, in [11], [12], [41], reinforcement learning was used to optimise the placement of machine learning models to improve throughput. In [14], model-based RL was used successfully to optimise the selection of bitrate when streaming data across a network. This work takes inspiration from prior work and we use model-based RL techniques to optimise deep learning models by reducing on-device runtime.

VI. CONCLUSION

We have shown the result of applying deep RL techniques to the task of optimising neural networks. Our approach uses RL agents to select optimal actions that apply sub-graph transformations to computation graphs with the goal of improving on-device runtime. We performed experiments that show RL agents decreased the runtime on all of the six test graphs, each of which had unique properties and architectures. We provided evidence to support our claim that it is possible to learn a world-model of the environment which is sufficiently accurate to enable the end-to-end training of an agent inside a fully imagined world-model.

In addition, this work has highlighted that the performance of model-based agents trained inside a hallucinogenic is highly

dependent on the accuracy of the world-model. Inaccuracies in the model, can lead to compounding errors and thus the agent choosing sub-optimal, or invalid, actions that diverges the imagined state from the true environment state. Hence, there are still significant fundamental difficulties in training stable, accurate world-models that can simulate the true environment; if one can train such a model by carefully tuning hyperparameters, we can gain substantial benefits through increased sample efficiency and decreased training time.

REFERENCES

- [1] M. Abadi, A. Agarwal, P. Barham, E. Brevdo, Z. Chen, C. Citro, G. S. Corrado, A. Davis, J. Dean, M. Devin, S. Ghemawat, I. Goodfellow, A. Harp, G. Irving, M. Isard, Y. Jia, R. Jozefowicz, L. Kaiser, M. Kudlur, J. Levenberg, D. Mané, R. Monga, S. Moore, D. Murray, C. Olah, M. Schuster, J. Shlens, B. Steiner, I. Sutskever, K. Talwar, P. Tucker, V. Vanhoucke, V. Vasudevan, F. Viégas, O. Vinyals, P. Warden, M. Wattenberg, M. Wicke, Y. Yu, and X. Zheng, “TensorFlow: Large-scale machine learning on heterogeneous systems,” 2015, software available from tensorflow.org. [Online]. Available: <https://www.tensorflow.org/>
- [2] A. Paszke, S. Gross, F. Massa, A. Lerer, J. Bradbury, G. Chanan, T. Killeen, Z. Lin, N. Gimelshein, L. Antiga, A. Desmaison, A. Kopf, E. Yang, Z. DeVito, M. Raison, A. Tejani, S. Chilamkurthy, B. Steiner, L. Fang, J. Bai, and S. Chintala, “Pytorch: An imperative style, high-performance deep learning library,” in *Advances in Neural Information Processing Systems* 32. Curran Associates, Inc., 2019, pp. 8024–8035. [Online]. Available: <http://papers.nips.cc/paper/9015-pytorch-an-imperative-style-high-performance-deep-learning-library.pdf>
- [3] NVIDIA, “Tensorrt: Programmable inference accelerator,” <https://developer.nvidia.com/tensorrt>, 2017.
- [4] T. Chen, T. Moreau, Z. Jiang, L. Zheng, E. Yan, M. Cowan, H. Shen, L. Wang, Y. Hu, L. Ceze, C. Guestrin, and A. Krishnamurthy, “Tvm: An automated end-to-end optimizing compiler for deep learning,” 2018.
- [5] Z. Jia, O. Padon, J. Thomas, T. Warszawski, M. Zaharia, and A. Aiken, “Taso: Optimizing deep learning computation with automatic generation of graph substitutions,” in *Proceedings of the 27th ACM Symposium on Operating Systems Principles*, ser. SOSP ’19. New York, NY, USA: Association for Computing Machinery, 2019, p. 47–62. [Online]. Available: <https://doi.org/10.1145/3341301.3359630>
- [6] R. Bellman, “A Markovian Decision Process,” *Journal of Mathematics and Mechanics*, vol. 6, no. 5, pp. 679–684, 1957. [Online]. Available: <http://www.jstor.org/stable/24900506>
- [7] V. Mnih, K. Kavukcuoglu, D. Silver, A. Graves, I. Antonoglou, D. Wierstra, and M. Riedmiller, “Playing atari with deep reinforcement learning,” *arXiv preprint arXiv:1312.5602*, 2013.
- [8] L. Kaiser, M. Babaeizadeh, P. Milos, B. Osinski, R. H. Campbell, K. Czechowski, D. Erhan, C. Finn, P. Kozakowski, S. Levine, A. Mohiuddin, R. Sepassi, G. Tucker, and H. Michalewski, “Model-based reinforcement learning for atari,” 2020.
- [9] D. Silver, T. Hubert, J. Schrittwieser, I. Antonoglou, M. Lai, A. Guez, M. Lanctot, L. Sifre, D. Kumaran, T. Graepel, T. Lillicrap, K. Simonyan, and D. Hassabis, “Mastering chess and shogi by self-play with a general reinforcement learning algorithm,” 2017.
- [10] OpenAI, I. Akkaya, M. Andrychowicz, M. Chociej, M. Litwin, B. McGrew, A. Petron, A. Paino, M. Plappert, G. Powell, R. Ribas, J. Schneider, N. Tezak, J. Tworek, P. Welinder, L. Weng, Q. Yuan, W. Zaremba, and L. Zhang, “Solving rubik’s cube with a robot hand,” 2019.
- [11] R. Addanki, S. B. Venkatakrishnan, S. Gupta, H. Mao, and M. Alizadeh, “Placeto: Learning generalizable device placement algorithms for distributed machine learning,” *arXiv preprint arXiv:1906.08879*, 2019.
- [12] A. Mirhoseini, A. Goldie, H. Pham, B. Steiner, Q. V. Le, and J. Dean, “A hierarchical model for device placement,” in *International Conference on Learning Representations*, 2018.
- [13] D. Silver, A. Huang, C. J. Maddison, A. Guez, L. Sifre, G. Van Den Driessche, J. Schrittwieser, I. Antonoglou, V. Panneershelvam, M. Lanctot *et al.*, “Mastering the game of go with deep neural networks and tree search,” *Nature*, vol. 529, no. 7587, p. 484, 2016.
- [14] H. Brown, K. Fricke, and E. Yoneki, “World-models for bitrate streaming,” *Applied Sciences*, vol. 10, no. 19, 2020. [Online]. Available: <https://www.mdpi.com/2076-3417/10/19/6685>
- [15] J. Robine, T. Uelwer, and S. Harmeling, “Smaller world models for reinforcement learning,” 2021.
- [16] D. Ha and J. Schmidhuber, “Recurrent world models facilitate policy evolution,” pp. 2451–2463, 2018, <https://worldmodels.github.io>. [Online]. Available: <https://papers.nips.cc/paper/7512-recurrent-world-models-facilitate-policy-evolution>
- [17] J. Schulman, F. Wolski, P. Dhariwal, A. Radford, and O. Klimov, “Proximal policy optimization algorithms,” *arXiv preprint arXiv:1707.06347*, 2017.
- [18] V. Mnih, A. P. Badia, M. Mirza, A. Graves, T. Lillicrap, T. Harley, D. Silver, and K. Kavukcuoglu, “Asynchronous methods for deep reinforcement learning,” in *International Conference on Machine Learning*, 2016, pp. 1928–1937.
- [19] C. J. Watkins and P. Dayan, “Q-learning,” *Machine Learning*, vol. 8, no. 3–4, pp. 279–292, 1992.
- [20] G. Brockman, V. Cheung, L. Pettersson, J. Schneider, J. Schulman, J. Tang, and W. Zaremba, “Openai gym,” *arXiv preprint arXiv:1606.01540*, 2016.
- [21] M. Lanctot, E. Lockhart, J.-B. Lespiau, V. Zambaldi, S. Upadhyay, J. Pérolat, S. Srinivasan, F. Timbers, K. Tuyls, S. Omidshafiei, D. Hennes, D. Morrill, P. Muller, T. Ewalds, R. Faulkner, J. Kramár, B. D. Vylder, B. Saeta, J. Bradbury, D. Ding, S. Borgeaud, M. Lai, J. Schrittwieser, T. Anthony, E. Hughes, I. Danihelka, and J. Ryan-Davis, “OpenSpiel: A framework for reinforcement learning in games,” *CoRR*, vol. abs/1908.09453, 2019. [Online]. Available: <http://arxiv.org/abs/1908.09453>
- [22] J. Bai, F. Lu, K. Zhang *et al.*, “ONNX: Open Neural Network Exchange,” <https://github.com/onnx/onnx>, 2019.
- [23] T. Chen, M. Li, Y. Li, M. Lin, N. Wang, M. Wang, T. Xiao, B. Xu, C. Zhang, and Z. Zhang, “Mxnet: A flexible and efficient machine learning library for heterogeneous distributed systems,” 2015.
- [24] M. Schuster and K. Paliwal, “Bidirectional recurrent neural networks,” *IEEE Transactions on Signal Processing*, vol. 45, no. 11, pp. 2673–2681, 1997.
- [25] A. Graves, “Generating sequences with recurrent neural networks,” 2014.
- [26] G. Hinton, O. Vinyals, and J. Dean, “Distilling the knowledge in a neural network,” 2015.
- [27] N. Hansen, “The cma evolution strategy: A tutorial,” 2016.
- [28] D. Hafner, T. Lillicrap, J. Ba, and M. Norouzi, “Dream to control: Learning behaviors by latent imagination,” 2020.
- [29] D. Hafner, T. Lillicrap, M. Norouzi, and J. Ba, “Mastering atari with discrete world models,” 2021.
- [30] P. W. Battaglia, J. B. Hamrick, V. Bapst, A. Sanchez-Gonzalez, V. Zambaldi, M. Malinowski, A. Tacchetti, D. Raposo, A. Santoro, R. Faulkner, C. Gulcehre, F. Song, A. Ballard, J. Gilmer, G. Dahl, A. Vaswani, K. Allen, C. Nash, V. Langston, C. Dyer, N. Heess, D. Wierstra, P. Kohli, M. Botvinick, O. Vinyals, Y. Li, and R. Pascanu, “Relational inductive biases, deep learning, and graph networks,” 2018.
- [31] C. Szegedy, V. Vanhoucke, S. Ioffe, J. Shlens, and Z. Wojna, “Rethinking the inception architecture for computer vision,” 2015.
- [32] K. He, X. Zhang, S. Ren, and J. Sun, “Deep residual learning for image recognition,” 2015.
- [33] F. N. Iandola, S. Han, M. W. Moskewicz, K. Ashraf, W. J. Dally, and K. Keutzer, “Squeezenet: Alexnet-level accuracy with 50x fewer parameters and <0.5mb model size,” 2016.
- [34] J. Devlin, M.-W. Chang, K. Lee, and K. Toutanova, “Bert: Pre-training of deep bidirectional transformers for language understanding,” 2019.
- [35] P. Nayak, “Understanding searches better than ever before,” <https://blog.google/products/search/search-language-understanding-bert>, 2019.
- [36] A. Dosovitskiy, L. Beyer, A. Kolesnikov, D. Weissenborn, X. Zhai, T. Unterthiner, M. Dehghani, M. Minderer, G. Heigold, S. Gelly, J. Uszkoreit, and N. Houlsby, “An image is worth 16x16 words: Transformers for image recognition at scale,” 2021.
- [37] H. Wang, J. Zhai, M. Gao, Z. Ma, S. Tang, L. Zheng, Y. Li, K. Rong, Y. Chen, and Z. Jia, “Pet: Optimizing tensor programs with partially equivalent transformations and automated corrections,” in *15th {USENIX} Symposium on Operating Systems Design and Implementation ({OSDI} 21)*, 2021, pp. 37–54.

- [38] Z. Jia, J. Thomas, T. Warszawski, M. Gao, M. Zaharia, and A. Aiken, "Optimizing dnn computation with relaxed graph substitutions," *SysML 2019*, 2019.
- [39] T. Weber, S. Racanière, D. P. Reichert, L. Buesing, A. Guez, D. J. Rezende, A. P. Badia, O. Vinyals, N. Heess, Y. Li, R. Pascanu, P. Battaglia, D. Hassabis, D. Silver, and D. Wierstra, "Imagination-augmented agents for deep reinforcement learning," 2018.
- [40] V. Feinberg, A. Wan, I. Stoica, M. I. Jordan, J. E. Gonzalez, and S. Levine, "Model-based value estimation for efficient model-free reinforcement learning," 2018.
- [41] A. Paliwal, F. Gimeno, V. Nair, Y. Li, M. Lubin, P. Kohli, and O. Vinyals, "Reinforced genetic algorithm learning for optimizing computation graphs," 2020.